



OPTIMIZING THE PERFORMANCE OF STATE ESTIMATION IN POWER SYSTEMS USING A NOVEL SWARM-INTELLIGENT APPROACH

Umesh Kumar Singh¹
Ramachandran T.
Mohit Kumar Sharma

Received 12.04.2023.

Accepted 20.06.2023.

Keywords:

Power system, state estimation, catagonyfly optimization (CFO), dragonfly algorithm (DA), IEEE-118 test environment.

ABSTRACT

For power systems to operate reliably and effectively, state estimate is essential. For monitoring and control applications, it offers real-time estimates of the system's state indicators, including voltage levels and orientations. In this paper, a novel catagonyfly optimization (CFO) technique that aims to improve state estimation effectiveness in electrical systems is presented. The suggested strategy combines optimization techniques from cat swarm and dragonfly. The suggested strategy is evaluated using the IEEE-118 test environment under various simulated scenarios, and the findings are contrasted with those of other methods already in use. The optimization results and statistical error assessment demonstrate the suggested CFO technique's efficiency to the alternatives. The results of this study also have the potential to improve the incorporation of sustainable energy sources, microgrids, and additional emerging innovations into existing power grids.



© 2023 Published by Faculty of Engineering

1. INTRODUCTION

The reliable operation and control of power systems are crucial for maintaining a stable and efficient supply of electrical energy. State estimation plays a fundamental role in power system operations, providing accurate and timely information about the system's operating conditions. It involves estimating the states of various components, such as voltages, currents, and power flows, based on available measurements (Impram et al., (2020)). State estimation serves as a vital tool for system monitoring, control, and planning, enabling operators to make informed decisions to ensure the overall stability and reliability of the power grid. As power systems continue to evolve and incorporate increasing levels of renewable energy sources, distributed

generation, and complex control systems, the challenges associated with accurate state estimation become more pronounced (Aziz et al., (2019)). Traditional state estimation methods, such as the weighted least squares approach, have been widely used and have proven effective in many scenarios. However, they may encounter limitations when dealing with large-scale power systems with nonlinearities, uncertainties, and dynamic changes. To address these challenges and optimize the performance of state estimation in power systems, researchers have been exploring innovative approaches that leverage advanced optimization techniques, machine learning algorithms, and data-driven methodologies. These approaches aim to enhance the accuracy, efficiency, and robustness of state estimation, ultimately improving the reliability and

¹ Corresponding author: Umesh Kumar Singh
Email: umeshsingh11feb@gmail.com

operational performance of power systems (Colbertaldo et al., (2019)). One prominent direction in optimizing state estimation performance is the utilization of advanced optimization algorithms (Ammari et al., (2022)).

These algorithms are designed to search for the best solution within a given solution space by iteratively adjusting the estimated states based on the measurements and system constraints. Evolutionary algorithms, such as genetic algorithms and particle swarm optimization, have shown promise in improving the accuracy and convergence speed of state estimation (Zhang et al., (2019)). By mimicking the natural process of evolution or the collective behavior of swarms, these algorithms are capable of exploring complex solution spaces and finding optimal or near-optimal solutions. In addition to optimization algorithms, machine learning techniques have emerged as powerful tools for state estimation optimization. By leveraging historical data and advanced data analytics approaches, machine learning algorithms can learn the underlying patterns and relationships in power system measurements to improve state estimation accuracy (Wang et al., (2020)).

Techniques such as artificial neural networks, support vector machines, and deep learning models have been applied to state estimation tasks, demonstrating their ability to handle complex nonlinearities and uncertainties in power systems. Furthermore, the integration of advanced measurement technologies, such as synchrophasors, has opened up new possibilities for enhancing state estimation accuracy and enabling real-time monitoring and control of power systems. Synchrophasor measurements provide high-resolution data about voltage and current waveforms, enabling more precise estimation of system states and better identification of dynamic behaviors (Ding et al., (2020)).

State estimation is crucial for the successful and dependable operation of power systems. It provides real-time estimates of the system's state indicators, such as voltage levels and orientations, for monitoring and control applications. In this paper, proposed approach is aims to improve state estimation effectiveness in electrical system are presented.

The remainder of this paper is arranged as follows: Part 2-related work, while part 3-materials and methods, Part 4-Result and discussion, and part 5-conclusion.

2. RELATED WORKS

Zhang et al., (2019) based on the real-time monitoring (estimation and forecasting) of power systems was one of the many areas that were addressed by data-driven advances made to DNN. The invention of prox-linear nets, which were utilized for power system state estimation (PSSE), was made possible as a result of the combination of neural networks (NNs) and more conventional physics-based optimization algorithms.

Using information from the past in conjunction with deep recurrent neural networks, which are more commonly referred to as RNNs, it is now able to provide accurate forecasts regarding the voltage of power systems. Their model-specific prox-linear net-based PSSE can be trained in a short amount of time and does not require a significant amount of computer resources to execute.

It is possible to achieve optimal performance with an organic rankine cycle (ORC) system by selecting the system variables as well as the working fluid simultaneously. An issue of this nature is referred to as mixed-integer non-linear programming (MINLP), which is an acronym. The CoMT-CAMD optimization method has been streamlined into a single stage after previously requiring multiple processes to complete. The purpose of optimization was to achieve certain goals, one of which was to maximize the amount of net power generation while simultaneously minimizing the temperature at the outlet that was caused by the heat source (Schilling et al., (2017)).

Akrami et al., (2021) proposes a one-of-a-kind sparse tracking DSSE system that is capable of overcoming the obstacle of poor observability in power distribution networks that only comprise a few D-PMUs. Specifically, this system is designed to function with networks that include a small number of D-PMUs. This method offers an original approach to solving the issue. The investigation is carried out with the assistance of differential synchrophasors, and the state variables are separated into four groups according to the level of group sparsity that is proven by each variable on an individual basis.

Jovicic et al., (2020) provided new circuit models to give a thorough modeling framework for the previously announced ECF-based state estimators. For various combinations of conventional tests, new models are generated. Additionally, a circuit representation with null injections and measurement-free buses is shown.

The dynamic state estimation issue for an islanded microgrid susceptible to fading observations has been addressed. It has been determined how to create a model of the isolated microgrid that incorporates fading measures and caters to a more realistic engineering environment. A set of stochastic parameters with established distributions of probability has been used to characterize the way to measure fading phenomenon (Qu et al., (2020)).

Zargar et al., (2020) introduced a new technique to placing PMUs to find the best balance between the quantity of PMUs and the intended level of estimating precision in a stochastic multi-objective framework. When PMUs are unable to access the full power system, the state estimator nonetheless makes an estimate using data from both traditional observations and PMUs.

Fang et al., (2021) proposed a grid that uses both direct current and alternating current (AC/DC). The process begins with the development of precise and models of the AC/DC grid's elements that are practical for the state estimation usage. Next, state variables and measuring equations are derived, and finally, a unique robust estimate against control and measurement input errors is developed.

In order to ensure the safety of the state estimation problems for NCSs, a comprehensive investigation was conducted. In order to portray the scenario in which fraudulent data are inserted in the registers for the communication channels and the estimator, an innovative idea for a joint-FDI assault was devised. When developing FDI attacks, designers made sure to take into account a number of limits, including limited access to resources and capacity for those resources. It has been discovered that the presence of malicious attack sequences that are capable of causing endless mistakes in estimation while evading the anomaly detection is one of the required and sufficient requirements for the system's sensitivity to various types of attack scenarios. This condition was determined to be both necessary and sufficient (Xu et al., (2021)).

3. MATERIALS AND METHODS

3.1 Dragonfly Algorithm

The distinct and improved swarming behavior of dragonflies inspires the Dragonfly Algorithm. Dragonfly swarms' behavior includes both travel and hunting. Let's say there are M dragonflies in the world. Eq. (1) states where N dragonfly is located.

$$W_j = (w_j^1, w_j^c, \dots, w_j^M) \quad (1)$$

While $i = 1, 2, 3, \dots, M$ and M indicate the number of search agents, w_j^c indicates where the j^{th} dragonfly is located in the c^{th} searchable dimension.

The fitness function, which is constructed arbitrarily between the highest and lowest limits of parameters, is estimated based on the initial location readings. Each dragonfly has a unique beginning value for the variables T (separation weight), c (cohesion), b (alignment), e (food), and f (opponent factors). Based on Eq. (2) to (4), factors for updating the velocity and location of dragonflies are computed.

$$T_j = - \sum_{i=1}^M w - w_j \quad (2)$$

$$B_j = \frac{\sum_{i=1}^M U_j}{M} \quad (3)$$

$$A_j = \frac{i=1}{M} - w \quad (4)$$

U_j and W_j Indicate the velocity and position of the j^{th} person, respectively. N denotes a group of nearby individuals, and U_j is the current position of the

individual. The EQ. (5) and (6) explain how to calculate E_j , which stands for Attraction towards a food source, and F_j , which stands for Distraction from Opponents.

$$F_j = W^+ - W \quad (5)$$

$$F_j = W^- + W \quad (6)$$

While W denotes the player's current location, W^- denotes the enemy source, and W^+ denotes the food source. To determine how far apart N dragonflies are from one another, we use the Euclidean distance between all of them. Distance, denoted by q_{ji} , is found with Eq. (7).

$$q_{ji} = \sqrt{\sum_{l=1}^c (w_{j,l} - w_{i,l})^2} \quad (7)$$

The location of the dragonfly will be updated based on Eq. (9) which is equivalent to the location formulation of PSO. This will be done on the basis of Eq. (8) which is analogous to the velocity formulation of PSO.

$$\Delta W_{s+1} = (tT_j + bB_j + cC_j + eE_j + fF_j) + x\Delta W_s \quad (8)$$

$$W_{s+1} = W_s + \Delta W_{s+1} \quad (9)$$

In the surrounding area, the dragonfly position will be modified using the Levy Flight equation, which can be found in Eq. (10). This will take place if there is no dragonfly radius. This makes the behavior of dragonflies even more arbitrary and unpredictable, while also increasing their capacity for global search.

$$W_{s+1} = W_s + \text{levy}(c)W_s \quad (10)$$

After then, the updated velocities and position are used to calculate the fitness function.

3.2 Cat swarm Optimization Algorithm (CSOA)

Cats' ability to relax and hunt is the foundation of CSOA. The "seeking mode" (SM) and "tracing mode" (TM) are models for these abilities. Even though the cat spends the majority of SM resting, it is constantly in an alert position. The cat is slow-moving in SM. Cats are much more active in TM than they are in SM, chasing their prey with great speed and vigor.

Seeking mode CSOA: Four parameters are employed in SM. There are "seeking memory pool (SMP), seeking range of the selected dimension for mutation (SRD), count of dimension to change (CDC), and self position consideration (SPC)". A mixture ratio (MR) is also taken to limit the number of cats in SM and TM. Below are listed the stages of SM;

Stage 1: As seeking cats, pick a random MR proportion of the population.

Stage 2: For each cat in SM, repeat stage 3-6.

Stage 3: Make i^{th} searching cat SMP duplicates.

Stage 4: Execute the following operations based on the value of CDC.

- SRD portion of the current position value should be added or subtracted at random for every single duplicate of the *ith* cat.
- For every duplicate, swap out the previous values.

Stage 5: Determine every duplicate's fitness.

Stage 6: Choose the duplicate that is the most suited among the duplicates, and then move it to the position of the seeker.

Tracing mode: Throughout TM, cats update their position and velocity in accordance with the best position thus far in order to advance toward it. Following are the stage in tracing mode;

Stage 1: The cat's position's speed for each dimension

Stage 2: If the updated speed is outside of the range, it is adjusted to the limits.

Stage 3: The cats' locations are updated.

Stage 4: Positions are adjusted to the limit if they are outside of the limited range.

$$u_i^c(s+1) = x \times u_i^c(s) + d \times q \times (w_{best}^c(s) - w_i^c(s)) \quad (11)$$

$$w_i^c(s+1) = w_i^c(s) + u_i^c(s+1) \quad (12)$$

Here $u_i^c(s)$ and $u_i^c(s+1)$ represent the speeds in dimension *c* of the cat at times *s* and *s+1*, respectively. $w_i^c(s)$ and $w_i^c(s+1)$ represent a position of the *c*th dimension of the *l*th cat at times *s* and *s+1*, *d* constant called *c* impact variations in speed of every dimension, whereas *r* is a random value between [0,1], and $w_{best}^c(s)$ is the location of *c*th dimensions of the cat ever found. *x* is inertia weight.

3.3 Catagonyfly Optimization

Any optimization strategy must strike the ideal balance between exploitation and exploration of the search space to arrive at a global solution. When searching for an ideal solution, exploitation, also known as intensification, narrows in on a small area around the current one, while exploration, also known as diversification, broadens the search to encompass the entire search space.

Excessive exploitation and exploration negatively impact the performance of the technique by lengthening the convergence time and increasing the likelihood that local optima will be reached. The existing DA uses Levy flight dragonflies to explore the search space along with an initially formed population of agents of search that was produced arbitrarily. This randomization and levy fly search technique increase the variety of solutions and strengthen the exploration capacity of the approach.

Additionally, DA only has a few controllable parameters, and the adaptive tuning of these swarming elements helps to strike a balance between the capabilities of global and local search. Nevertheless,

DA does not possess an internal memory that is able to keep a record of previously accomplished potential solutions. When the method is being executed, DA steers clear of any fitness values that are higher than the global optimal and does not remain on the set of likely solutions that can converge to the global optimal. This makes it more difficult for the DA attention to gradually converge, and it also makes it more likely that it will become inactive at local optimums. A strategy that is based on the CSOA and DA is developed in order to circumvent that obstacle.

$$u_i^c(s+1) = x \times u_i^c(s) + d \times q \times (DA - w_{best}^c(s) - w_i^c(s)) \quad (13)$$

$$w_i^c(s+1) = w_i^c(s) + u_i^c(s+1) \quad (14)$$

3.4 Bad data assessment

The proposed approach has been used in this paper for its great efficiency in the identification and detection of incorrect data.

$$O = G(G^S Q^{-1} G) G^S Q^{-1} \quad (15)$$

$$q = \Delta y - \Delta \hat{y} = \Delta y - O \Delta y = (J_{JN} - O) \Delta y = T \Delta y \quad (16)$$

The residual sensitivity matrix is denoted by the symbol $T (= J_{JN} - O)$. The matrix of identity J_{JN} has the same number of rows and columns as *G*, and *f* is the complex sound vector. The operator that maps Δy to the Jacobian space of measurements, $(Q(Z)^\perp)$, is the *T* matrix.

For the *i*th measurement vector, which is $n_j = N_j \delta_j$ with $\delta_j = [0 \dots 1^j \dots 0]^S$ and N_j being the magnitude of the measurement value *i*, the two measuring elements are discovered to be $N_{jQ(Z)} = O(N_j \delta_j)$ and $N_{jQ(Z)^\perp} = (J_{JN} - O)(N_j \delta_j)$. Consequently, the inventive index (N_{jQ}) is determined as

$$N_{jQ} = \|N_{jQ(Z)^\perp}\| X / \|N_{jQ(Z)}\| X \quad (17)$$

To determine the presence of faulty data, the biggest component *N*th in N_{jQ} is contrasted to a statistical threshold, $\xi (=0.250)$. The value of the index of the greatest element yields the index of faulty measurement data. When erroneous information is detected and corrected, the measurement results should be corrected. The following equation can be used to determine the normalized error in the adjusted measurements,

$$\|f_{n_j}\|^2 = (1 + 1/I_j^2) q_j^2 \quad (18)$$

q_j denotes the measurement of the *i* residual,

A substantial and unexpected change in load could happen in a power system. It is crucial to distinguish between a rapid, significant shift in load and the existence of faulty data in measurements. An index known as the asymmetry index (AI) has been employed for this differentiation. As defined by AI,

$$|\gamma_l| = N_{3,l} / \sigma_l^3 \quad (19)$$

Where $N_{3,l}$ denotes the third moment of the discrimination at time s_l and σ_l is the standard deviation of the distribution at s_l . If γ_l is greater than a pre defined value (here γ_{max}), then measurements are with gross errors and if $|\gamma_l|$ is less than $|\gamma_{max}|$ large load change occurred is considered.

4. RESULT AND DISCUSSION

IEEE test systems 118- bus 53PV buses, 186 lines, 64 PQ buses, 36.78 P_D , 14.38 Q_D , 9 transformer tapings, 14 shunt capacitances and 607 measurements.

The performance of the recommended SE approaches was evaluated using multiple performance indicators and contrasted to that of the WLS method under both regular operation and faulty data collection conditions. And the average absolute state error (AASE) is determine as

$$AASE(l) = \frac{1}{2*(MA-1)} \sum_{j=1}^{2*(MA-1)} (\hat{w}_j(l) - w_j^s(l)) \quad (20)$$

Where $w(\cdot)$ is the state vector, consisting of magnitudes and angles of phase is $U(\cdot)$. $\hat{w}(l)$ and w_j^{sq} are the state vector's projected value and true measurement value at l th time step. The performance index $J(K)$ is calculated as

$$J(l) = \frac{\sum_{j=1}^{Mn} |\hat{y}_j(l) - y_j^s(l)|}{\sum_{j=1}^{Mn} |\hat{y}_j(l) - y_j^s(l)|} \quad (21)$$

Where $\hat{y}(l)$, $y(l)$ and $y^s(l)$ demonstrates the measured and actual values of the measurements, and m denotes the number of measures employed. Table 2 shows that different value ranges of the objective function for the IEEE 118-bus test system with various approaches.

Table 1. A description of the lower value ranges of the objective for test system.

Test system		IEEE 118-bus		
Optimization method		PSO	GSA	CFO
Range 1	Min	15.5266	0.3001	0.5025
	Max	19.6483	0.3157	0.5237
	$M.D^a$	4.1917	0.1256	0.0912
	$F.O^a$	70	78	77
Range 2	Min	19.5984	0.3058	0.5138
	Max	23.8001	0.4174	0.4950
	$M.D^a$	4.2017	0.1156	0.1212
	$F.O^b$	16	14	21
Range 3	Min	23.7802	0.3375	0.5051
	Max	27.9419	0.3911	0.5163
	M.D	4.1617	0.0556	0.0112
	F.O	9	6	4
Range 4	Min	27.8920	0.4312	0.4864
	Max	32.0937	0.5148	0.6176
	M.D	4.2117	0.1156	0.2012
	F.O	7	5	2

Maximum of mean square error (MMSE) is a common measure for estimating the quality of a dependent variable's fitted values as follows;

$$MMSE = \max \left[\frac{1}{MS} \sum_{l=1}^{MT} \{ \hat{w}_j(l) - w_j^s(l) \}^2 \right] \forall j \quad (22)$$

Maximum of standard deviation error (MSDE) calculates a population's variability over various samples as follows;

$$MSDE = \max \left[\frac{1}{(MS-1)} \sum_{l=1}^{MT} \{ \hat{w}_j(l) - w_j^s(l) \}^2 \right]^{0.5} \forall j \quad (23)$$

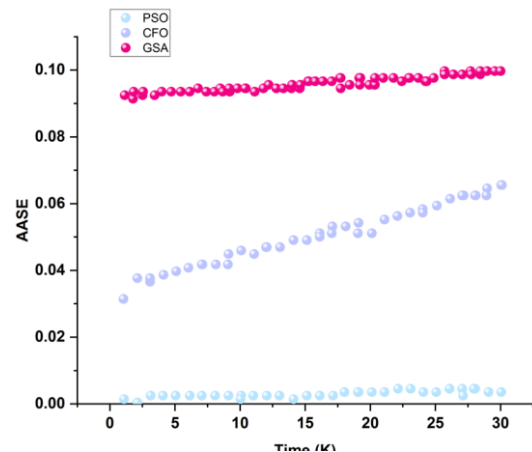


Figure 1. AASE(l) obtained comparison by GSA, PSA and CFO for 118-bus

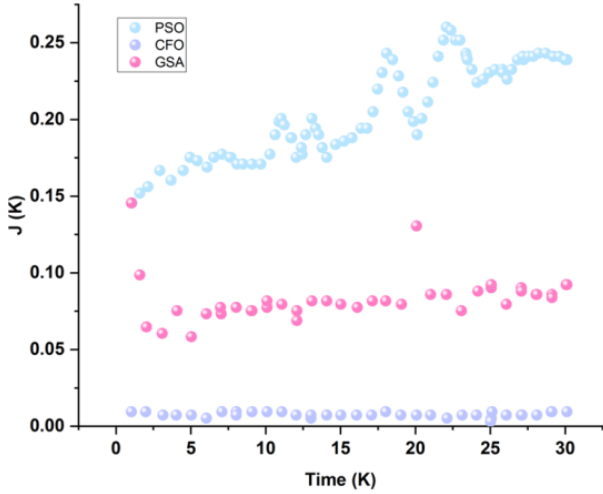


Figure 2. $J(l)$ Obtained comparison GSA, PSA and CFO for 118-bus

In, Figures 1 and 2 $AASE(l)$ and $J(l)$ denotes the 118-bus test has been proposed, From Figure 1 $AASE(l)$ obtained, the proposed method CFO is nearest to zero then all techniques. So, that depicts proposed method CFO is more accurate than existing methods GSA and PSO. $J(l)$ Presented figure 2 displays, the existing approaches GSA is close to 0.05 and PSO close to 0.1 while proposed method closest to 0. So, it is obvious that proposed method is more accuracy in $J(l)$ obtained graph than existing methods.

Figure 3 shows that statistical parameters, by load variation from 75% to 115% of base load for 118-bus test both with and without bad data assessment. The performance indicates that the existing approach PSA has the worst performance while compared with other method's performance. The proposed method gives better performance in both with and without bad data than all other approaches which depicts in figure 3. Calculate for 118-bus to identify and eliminate the bad data from measurements shown in figure 4.

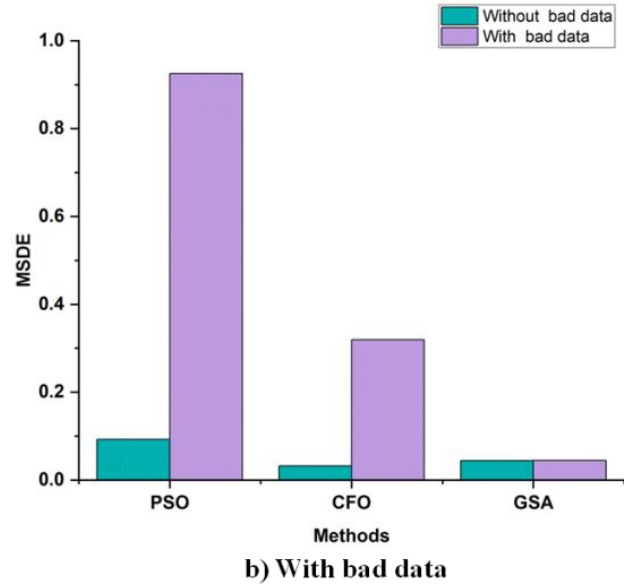


Figure 3. Statistical parameters for 118-bus (Load 75% to 115%)

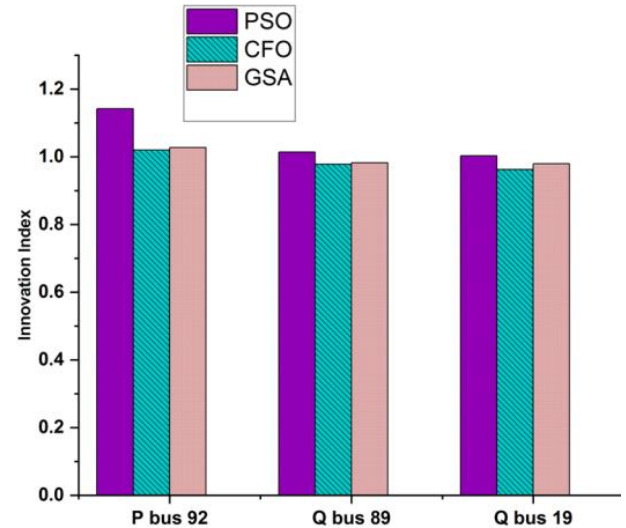
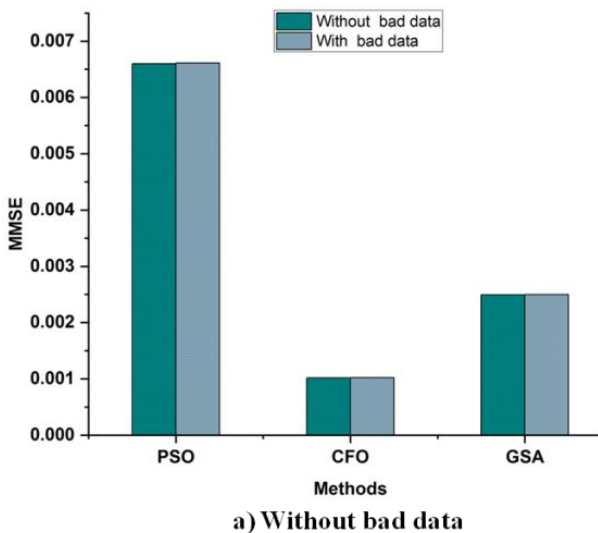


Figure 4. Measurements level of gross error



a) Without bad data

Figure 5 shows that comparison between the true values of voltage magnitude, active bus power, and reactive line flows attained in GSA, PSA and CFO of load 75% to 115% for bus 92 of 118-bus. The proposed method has better performance than all other methods.

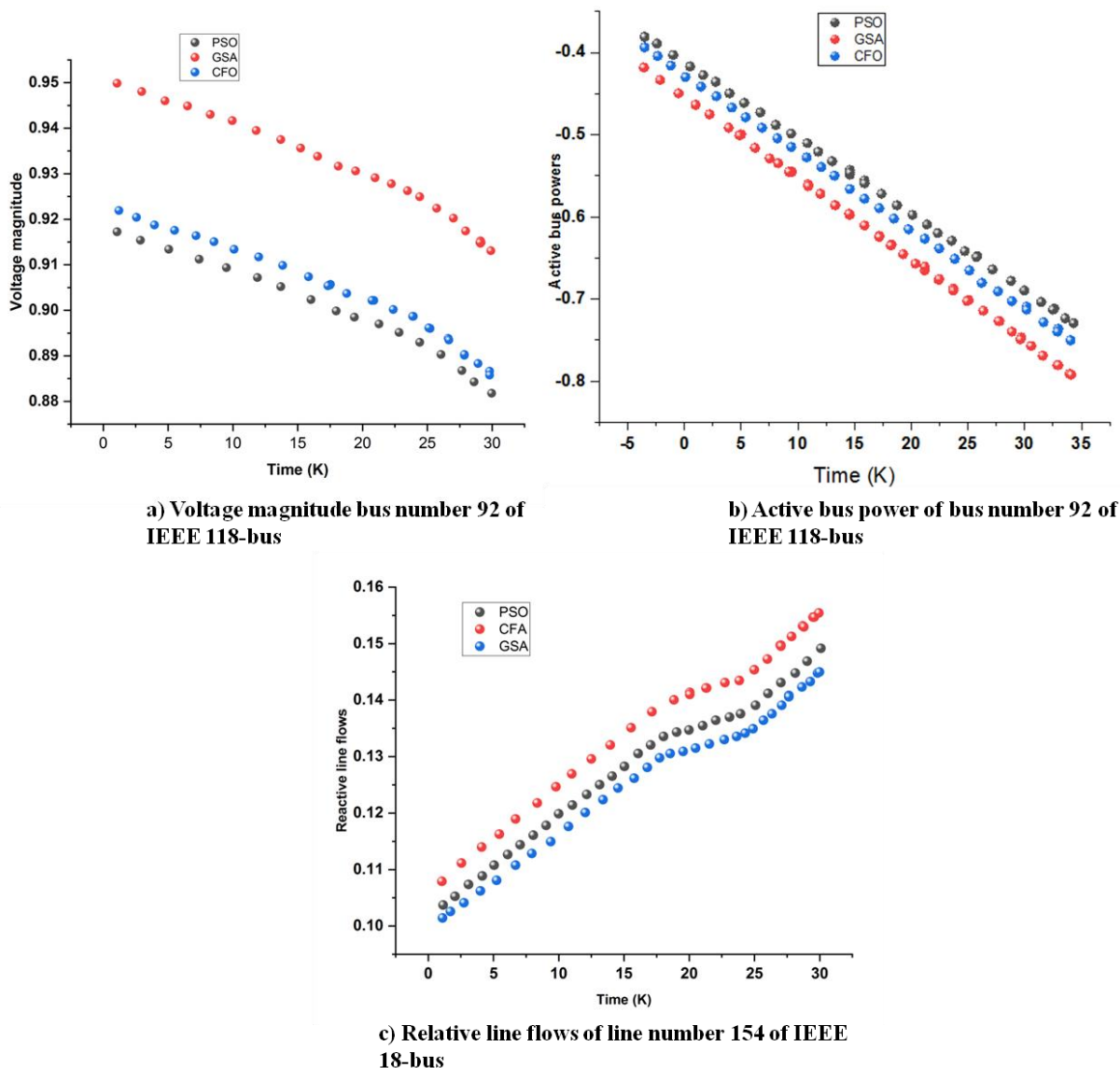


Figure 5. Results of voltage and power values of IEEE-118 system

5. CONCLUSION

In this paper, catagonly optimization (CFO) method which is combination of cat swarm and dragonfly optimization have been proposed. The proposed technique has been tested on standard IEEE-118 undervarious arrangements of the bad-data measurement conditions to evaluate the effectiveness of their optimization. The outcomes of the proposed method were contrasted with existing methods are PSO and GSA. When all comparison factors are

considered, the proposed approach demonstrates to be better suited for state estimation assessment with high accuracy than existing methods. And the limitation of optimization is due to the large number of factors and weights utilized in the position update, it has low level of stability. In the future, the focus of research will be on issues such as attack-defense game interactions, distributed detection based on AC power flow models, and assumptions that are more realistic.

References:

Akrami, A., Asif, S. and Mohsenian-Rad, H., 2021. Sparse tracking state estimation for low-observable power distribution systems using D-PMUs. *IEEE Transactions on Power Systems*, 37(1), pp.551-564. doi:<https://doi.org/10.1109/TPWRS.2021.3094534>

Ammari, C., Belatrache, D., Touhami, B. and Makhloufi, S., 2022. Sizing, optimization, control and energy management of hybrid renewable energy system—A review. *Energy and Built Environment*, 3(4), pp.399-411. doi:<https://doi.org/10.1016/j.enbenv.2021.04.002>

- Aziz, A.S., Tajuddin, M.F.N., Adzman, M.R., Azmi, A. and Ramli, M.A., 2019. Optimization and sensitivity analysis of standalone hybrid energy systems for rural electrification: A case study of Iraq. *Renewable energy*, 138, pp.775-792. doi:https://doi.org/10.1016/j.renene.2019.02.004
- Colbertaldo, P., Agustin, S.B., Campanari, S. and Brouwer, J., 2019. Impact of hydrogen energy storage on California electric power system: Towards 100% renewable electricity. *International Journal of Hydrogen Energy*, 44(19), pp.9558-9576. doi:https://doi.org/10.1016/j.ijhydene.2018.11.062
- Ding, D., Wang, Z., Ho, D.W. and Wei, G., 2017. Distributed recursive filtering for stochastic systems under uniform quantizations and deception attacks through sensor networks. *Automatica*, 78, pp.231-240. doi:https://doi.org/10.1016/j.automatica.2016.12.026
- Fang, Z., Lin, Y., Song, S., Li, C., Lin, X., Wang, F. and Lu, Y., 2021. A comprehensive framework for robust AC/DC grid state estimation against measurement and control input errors. *IEEE Transactions on Power Systems*, 37(2), pp.1067-1077. doi:https://doi.org/10.1109/TPWRS.2021.3105391
- Impram, S., Nese, S.V. and Oral, B., 2020. Challenges of renewable energy penetration on power system flexibility: A survey. *Energy Strategy Reviews*, 31, p.100539. doi:– 10.18421/IJQR12.02-10
- Jovicic, A., Jereminov, M., Pileggi, L. and Hug, G., 2020. Enhanced modelling framework for equivalent circuit-based power system state estimation. *IEEE Transactions on Power Systems*, 35(5), pp.3790-3799. doi:https://doi.org/10.1109/TPWRS.2020.2974459
- Qu, B., Shen, B., Shen, Y. and Li, Q., 2020. Dynamic state estimation for islanded microgrids with multiple fading measurements. *Neurocomputing*, 406, pp.196-203. doi:https://doi.org/10.1016/j.neucom.2020.03.104
- Schilling, J., Lampe, M., Gross, J. and Bardow, A., 2017. 1-stage CoMT-CAMD: An approach for integrated design of ORC process and working fluid using PC-SAFT. *Chemical Engineering Science*, 159, pp.217-230. doi:https://doi.org/10.1016/j.egypro.2017.09.169
- Wang, C., Zhang, H. and Ma, P., 2020. Wind power forecasting based on singular spectrum analysis and a new hybrid Laguerre neural network. *Applied Energy*, 259, p.114139. doi:https://doi.org/10.1016/j.apenergy.2019.114139
- Xu, W., Wang, Z., Hu, L. and Kurths, J., 2021. State estimation under joint false data injection attacks: Dealing with constraints and insecurity. *IEEE Transactions on Automatic Control*, 67(12), pp.6745-6753. doi:https://doi.org/10.1109/TAC.2021.3131145
- Zargar, S.F., Farsangi, M.M. and Zare, M., 2020. Probabilistic multi- objective state estimation- based PMU placement in the presence of bad data and missing measurements. *IET Generation, Transmission & Distribution*, 14(15), pp.3042-3051. doi:https://doi.org/10.1049/iet-gtd.2019.1317
- Zhang, L., Wang, G. and Giannakis, G.B., 2019. Real-time power system state estimation and forecasting via deep unrolled neural networks. *IEEE Transactions on Signal Processing*, 67(15), pp.4069-4077. doi:https://doi.org/10.1109/TSP.2019.2926023
- Zhang, Z., Zhang, D. and Qiu, R.C., 2019. Deep reinforcement learning for power system applications: An overview. *CSEE Journal of Power and Energy Systems*, 6(1), pp.213-225. doi:https://doi.org/10.17775/CSEEJPES.2019.00920

Umesh Kumar Singh

Teerthanker Mahaveer University,
Moradabad, Uttar Pradesh, India
umeshsingh11feb@gmail.com
ORCID 0000-0002-3537-1894

Ramachandran T.

Jain (deemed to be) University,
Bangalore, India
t.ramachandran@jainuniversity.ac.in
ORCID 0000-0002-6991-0403

Mohit Kumar Sharma

Vivekananda Global University, Jaipur,
India
mohit.kumar.sharma@vgu.ac.in
ORCID 0000-0002-5680-9111
